



Koponen, Jonna, Davies, Christine, Donald, Gordon, Follana, Eduardo, Lepage, G. Peter, Na, Heechang, and Shigemitsu, Junko(2011) *The D to K and D to pi semileptonic decay form factors from Lattice QCD*. In: XXIX International Symposium on Lattice Field Theory - Lattice 2011, 10-16 July 2011, Squaw Valley, Lake Tahoe, CA, USA.

Copyright © 2011 The Authors

<http://eprints.gla.ac.uk/90924/>

Deposited on: 18 February 2014

Axial vector form factors in $D_s \rightarrow \phi$ semileptonic decays from lattice QCD

Gordon Donald*, Christine Davies and Jonna Koponen, the HPQCD Collaboration

SUPA, School of Physics and Astronomy, University of Glasgow, Glasgow G12 8QQ, UK

E-mail: g.donald@physics.gla.ac.uk

We calculate axial vector and vector form factors for the semileptonic decay $D_s \rightarrow \phi$ using HISQ valence quarks on MILC ensembles with $2+1$ flavours of asqtad sea quarks. Using twisted boundary conditions to tune the quarks' momenta, we compute form factors at $q^2 = 0$ on coarse lattices. We find $V(0) = 0.903(67)$, $A_1(0) = 0.603(20)$, $A_2(0) = 0.401(80)$ and $A_0(0) = 0.686(17)$, which we compare to experimental data and previous quenched lattice QCD calculations.

The XXIX International Symposium on Lattice Field Theory - Lattice 2011

July 10-16, 2011

Squaw Valley, Lake Tahoe, California

*Speaker.

1. Introduction

The decay rate for the semileptonic meson decay $D_s \rightarrow \phi l \nu$ contains nonperturbative QCD form factors, about which we obtain information from lattice QCD. The quark level transition is $c \rightarrow s$ and the decay is from a pseudoscalar meson to a vector.

Labelling the pseudoscalar as D_s with momentum p and the vector meson as ϕ with momentum p' and polarisation vector ε , the general form for a pseudoscalar to vector matrix element is [1]:

$$\begin{aligned} \langle \phi(p', \varepsilon) | V^\mu - A^\mu | D_s(p) \rangle = & \frac{2i\varepsilon_{\mu\nu\alpha\beta}}{m_{D_s} + m_\phi} \varepsilon^\nu p_{D_s}^\alpha p_\phi^\beta V(q^2) \\ & - (m_{D_s} + m_\phi) \varepsilon^\mu A_1(q^2) \\ & + \frac{\varepsilon \cdot q}{m_{D_s} + m_\phi} (p + p')^\mu A_2(q^2) \\ & + 2m_\phi \frac{\varepsilon \cdot q}{q^2} q^\mu A_3(q^2) \\ & - 2m_\phi \frac{\varepsilon \cdot q}{q^2} q^\mu A_0(q^2) \end{aligned} \quad (1.1)$$

where we have the relations

$$A_3(q^2) = \frac{m_{D_s} + m_\phi}{2m_\phi} A_1(q^2) - \frac{m_{D_s} - m_\phi}{2m_\phi} A_2(q^2) \quad (1.2)$$

and

$$A_3(0) = A_0(0). \quad (1.3)$$

$V(q^2)$ is the vector form factor. There are three independent axial vector form factors as $A_3(q^2)$ is just a combination of $A_1(q^2)$ and $A_2(q^2)$ and at $q^2 = 0$ there are only two. Calculating the form factors at $q^2 = 0$ allows us to compare to experiment for the experimentally accessible $A_1(q^2)$, $A_2(q^2)$ and $V(q^2)$ form factors. BaBar [3] quote results for the quantities $r_2 = \frac{A_2(0)}{A_1(0)}$ and $r_V = \frac{V(0)}{A_1(0)}$.

2. Methods

2.1 Lattice setup

To compute semileptonic form factors, we calculate strange quark propagators using a random wall source on a timeslice at x . A strange quark propagates to the sink, y , and then is used to make an extended propagator in which a charm quark propagates back to the current insertion at z , which is summed over a timeslice. At the current insertion, the extended propagator is joined to the strange propagator to make the 3 point function.

We use HISQ [4] valence quarks, which means that suitable phases for staggered quarks have to be inserted at the source, sink and current insertion. The gauge configurations used are from MILC ensembles [5], which include 2+1 flavours of asqtad sea quarks. Currently we have performed calculations on only one ensemble, which has $\beta = 6.76$ and $V = 20^3 \times 64$, so $a \sim 0.12\text{fm}$. In general, the 3 point correlation function is

$$\langle \bar{\psi}(x) \gamma_\mu \psi(x') \bar{\psi}(z) \gamma_5 \gamma_\nu \psi(z') \bar{\psi}(y) \gamma_5 \psi(y') \rangle, \quad (2.1)$$

where we allow for point splitting at the source, sink and current insertion.

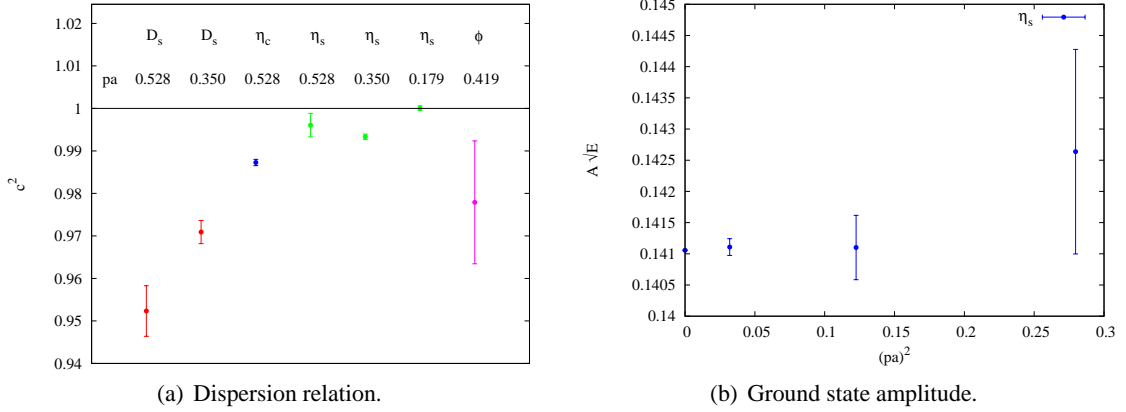


Figure 1: To check that introducing twisted boundary conditions gives us a physical momentum, we can calculate the speed of light for various mesons and momenta, $c^2 = \frac{E^2 - m^2}{p^2}$ (Fig. 1(a)) and look at the ground state's amplitude, A , as a function of meson energy. We expect $A\sqrt{E}$ to be constant (Fig. 1(b)).

	1-link	local	experiment
m_ϕ	1086(4) MeV	1083(4) MeV	1019 MeV
f_ϕ	248(4) MeV	233(13) MeV	227(4) MeV
	$Z = 1.095$	$Z = 0.97$	PDG $\Gamma_{e^+e^-}$

Table 1: The masses and decay constants for our ϕ mesons calculated using the 1-link and local vector operators. We include experimental values from the PDG [9] and note the lattice normalisation factors used for each calculation.

2.2 Twisted boundary conditions

To calculate the form factor at $q^2 = 0$, we use a ϕ with non-zero momentum and a D_s meson at rest. We use twisted boundary conditions [6, 7], where we insert a tunable phase, θ , at the boundary so $\psi(x + \hat{L}) = \psi(x)e^{i\theta}$. In Figure 1, we check that this introduces a physical momentum by looking at the dispersion relation and the amplitude of the ground state.

2.3 ϕ 2 point correlators

To extract matrix elements from 3 point correlators, we fit the 2 and 3 point functions simultaneously. The 2 point functions give us the masses and decay constants of the ϕ and D_s mesons in the 3 point amplitudes. The D_s mass is known to be accurately calculated with HISQ quarks [8]. We also extract m_ϕ and f_ϕ , using either a taste-singlet 1-link or local vector operator. Table 1 gives the masses and decay constants of the 1-link and local ϕ mesons, which are in agreement.

The ϕ meson is not gold-plated, which means that it can decay to $K\bar{K}$ with a small width, an effect we do not fully include. We have only done these calculations at one lattice spacing, so we cannot yet tell how much of the difference between the calculated lattice and continuum ϕ masses is caused by discretisation effects. With results on finer lattices, the effects of the non-gold-platedness of the ϕ can be studied in more detail. The normalisation factor for the 1-link vector operator is

from Ref. [10] and a perturbative normalisation is used for the local vector [11]. We extract f_ϕ from the PDG results for $\Gamma_{e^+e^-}$ [9], using

$$\Gamma_{e^+e^-} = \frac{4\pi}{3} \alpha_{QED}^2 e_Q^2 \frac{f_\phi^2}{m_\phi}. \quad (2.2)$$

2.4 Operator normalisation

2.4.1 1-link A_μ

To normalise the one link axial vector operator, we use simultaneous fits to

$$\langle \bar{\psi}(x) \gamma_5 \psi(x) \bar{\psi}(y) \gamma_5 \gamma_\mu \psi(y + \hat{\mu}) \rangle \text{ and } \langle \bar{\psi}(x) \gamma_5 \psi(x) \bar{\psi}(y) \gamma_5 \psi(y) \rangle, \quad (2.3)$$

making use of the facts that the operators $\bar{\psi}(x) \gamma_5 \psi(x)$ and $\bar{\psi}(x) \gamma_5 \gamma_\mu \psi(x + \hat{\mu})$ have the same taste and the pseudoscalar current is absolutely normalised.

The pseudoscalar and axial vector operators (in the continuum) can be related by

$$p_\mu \langle 0 | A_\mu | P_0 \rangle = (m_1 + m_2) \langle 0 | P | P_0 \rangle. \quad (2.4)$$

The fit output gives the amplitude for both the pseudoscalar and the axial vector operators, which we obtain for several values of the meson momentum. The ratio of amplitudes is a straight line against p_μ with a gradient of the Z factor times the appropriate mass combinations. In Figure 2, we plot this for various charm and strange pseudoscalar mesons. For cs , the current we need for $D_s \rightarrow \phi$, we obtain the value $Z = 1.065(5)$.

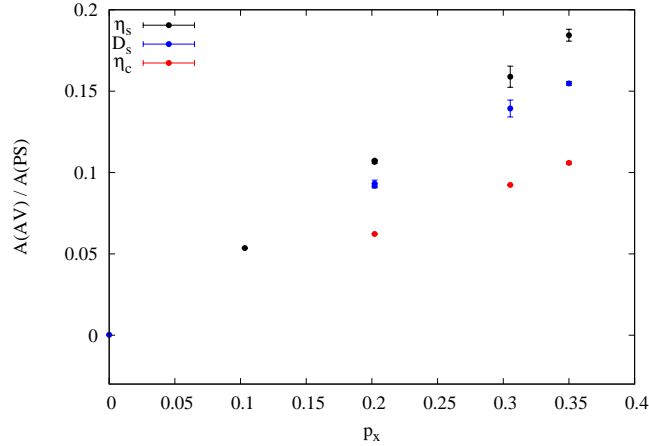


Figure 2: The ratio of amplitudes for the pseudoscalar and axial vector operators goes as $\frac{p_\mu}{Z} \frac{m_1 + m_2}{m_{P_0}^2}$, so the Z factors can be extracted from the gradients of these lines.

2.4.2 Local A_μ

We can normalise the local A_t component by creating non-Goldstone pseudoscalar mesons to compare to Goldstone mesons

$$\langle \bar{\psi}(x) \gamma_5 \gamma_t \psi(x) \bar{\psi}(y) \gamma_5 \gamma_t \psi(y) \rangle. \quad (2.5)$$

With HISQ, the masses are very close (for the D_s , the mass difference is 4.5 MeV) and the amplitudes, a_{NG} and a_G for the non-Goldstone and Goldstone mesons respectively, are related by

$$ZE_{D_s} a_{NG} = (m_c + m_s) a_G, \quad (2.6)$$

where we have included the Z factor for the local axial current. For cs , we obtain $Z = 1.036(4)$ for the local A_μ operator. Note that because the masses are so close, we can also use non-Goldstone D_s mesons in 3 point functions, which is useful when calculating the vector form factor, $V(q^2)$.

3. $D_s \rightarrow \phi$ form factors

3.1 $A_1(q^2)$ form factor

By setting up the ϕ polarisation and momentum such that $\varepsilon \cdot q = 0$, we can isolate the $A_1(q^2)$ form factor:

$$\langle \phi(p', \varepsilon) | A^\mu | D_s(p) \rangle = (m_{D_s} + m_\phi) \varepsilon^\mu A_1(q^2). \quad (3.1)$$

We can use either the 1-link or local operator for the ϕ source, along with the appropriate axial vector current insertion.

The determinations of the $A_1(q^2)$ form factor using both the local and 1-link operators are plotted in Figure 3, along with the other form factors for $D_s \rightarrow \phi$.

3.2 $V(q^2)$ form factor

We can extract the vector form factor, $V(q^2)$, using a vector current insertion from Equation (1.1) provided at least one of the D_s and ϕ mesons is not at rest. The 3 point function (with D_s at rest) is

$$\langle \bar{\psi}(x) \gamma_\mu \psi(x + \hat{\nu}) \bar{\psi}(z) \gamma_\alpha \psi(z) \bar{\psi}(y) \gamma_\nu \psi(y) \rangle = \frac{2i \varepsilon_{\mu\nu\alpha\ell}}{m_{D_s} + m_\phi} \varepsilon^\mu E_{D_s} p_\phi^\nu V(q^2), \quad (3.2)$$

where μ , ν and α are the three spatial directions. We use the non-Goldstone D_s so need only include one link of point splitting to obtain an overall taste-singlet three point correlator for the pseudoscalar to vector transition with a local vector current insertion.

We use a local vector normalisation of $Z = 1.021(2)$ which is obtained [10] by comparing a non-Goldstone $D_s \rightarrow \eta_s$ decay through a local temporal vector current to the Goldstone $D_s \rightarrow \eta_s$ with a (normalised) 1-link vector current. $V(q^2)$ is plotted in Figure 3.

3.3 $A_0(q^2)$ and $A_2(q^2)$ form factors

The form factor $A_0(q^2)$ can be extracted using the pseudoscalar density:

$$\begin{aligned} (m_c + m_s) \langle \phi(p', \varepsilon) | P | D_s(p) \rangle &= q_\mu \langle \phi(p', \varepsilon) | A^\mu | D_s(p) \rangle \\ &= 2m_\phi \varepsilon \cdot q A_0(q^2). \end{aligned} \quad (3.3)$$

The pseudoscalar form factor is not experimentally accessible, but is useful because it provides a route to obtaining $A_2(q^2)$.

We can use Equation (1.3) at $q^2 = 0$, $A_3(0) = A_0(0)$ to extract $A_2(0)$ from $A_0(0)$ and $A_1(0)$, although this does not hold at other values of q^2 . However we can calculate $\langle \phi(p', \varepsilon) | A_\mu | D_s(p) \rangle$ with $\varepsilon \cdot q \neq 0$ and use our determinations of $A_1(q^2)$ and $A_0(q^2)$ to find $A_2(q^2)$ with Equation (1.1), provided $\frac{1}{q^2}$ is not too large.

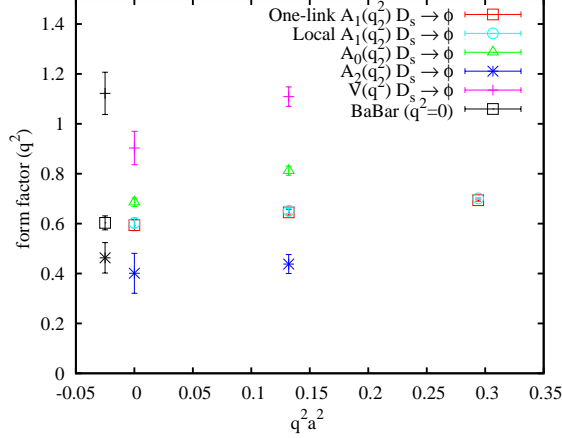


Figure 3: The form factors for $D_s \rightarrow \phi$. Because of the kinematics, only $A_1(q^2)$ contributes at q_{max}^2 (where both the D_s and ϕ mesons are at rest). All the form factors are calculated with $p_\phi a = 0.3$ and $p_\phi a = 0.4195$, where the latter corresponds to $q^2 = 0$. We also plot BaBar's values for the experimentally accessible $A_1(q^2)$, $A_2(q^2)$ and $V(q^2)$ form factors at $q^2 = 0$.

	HPQCD 2011	BaBar 2008 [3]	UKQCD 2001 [2]
$A_1(0)$	0.594(22)	0.607(11)(19)(18)	0.63(2)
Local $A_1(0)$	0.603(20)	—	—
$V(0)$	0.903(67)	1.122(85)*	0.85(4)
$A_0(0)$	0.686(17)	—	0.63(2)
$A_2(0)$	0.401(80)	0.463(61)*	0.62(5)
r_V	1.52(12)	1.849(60)(95)	1.35(7)*
r_2	0.62(12)	0.763(71)(65)	0.98(8)*

Table 2: Table of form factors at $q^2 = 0$. We quote our determinations of $A_1(0)$ using 1-link and local operators separately. Entries marked with * have been extracted from the published results. BaBar's results include statistical and systematic errors. The third error quoted on their value of $A_1(0)$ is from theoretical input.

3.4 Comparison with experiment and previous calculations

Table 2 compares our results at $q^2 = 0$ to BaBar's and those of previous quenched lattice QCD calculations. Our results for $A_2(0)$ and r_2 use our local $A_1(0)$ result, but the 1-link result is in close agreement. We calculate r_2 directly from our results for $A_1(0)$ and $A_0(0)$ for better control of the errors.

In Figure 3, we plot the shape of the form factors as a function of q^2 . We expect the q^2 dependence to be relatively mild, and approximately the same, for all the axial vector form factors and steeper for the vector form factor. BaBar assume the shape of the form factor and extract its value at $q^2 = 0$ from the total semileptonic rate. Our results for $A_1(0)$ and $A_2(0)$ are in agreement with BaBar and our $V(0)$ result is a little lower. In the previous quenched lattice QCD results, no

difference was found between $A_1(0)$, $A_2(0)$ and $A_0(0)$. It is clear from Figure 3 that our results are different for these form factors at $q^2 = 0$.

3.5 Future work

To understand the discretisation effects better and also the importance of the non-gold-platedness of the ϕ mesons, we intend to repeat our calculations on MILC fine configurations, along with the determination of the Z factors and semileptonic matrix elements. We will also look at using lighter sea quark masses as, although neither the ϕ nor the D_s contain light valence quarks, the non-gold-platedness of the ϕ may be an issue.

The $V(q^2)$ form factor is also important for radiative decays, where the photon is coupled by a vector operator, such as $J/\psi \rightarrow \eta_c \gamma$. We will calculate this with the same method used here for $D_s \rightarrow \phi$.

We can extend our axial vector form factor calculations to heavier quarks. Using HISQ for the heavy quark, we will extrapolate to the b quark mass [12] and calculate quantities such as $A_1(q_{max}^2)$ for $B \rightarrow D^*$.

Acknowledgements

We are grateful to the MILC collaboration for the use of their configurations. This work was funded by STFC. The calculations were performed at the High Performance Computing Centre in Cambridge as part of the DiRAC facility, jointly funded by STFC, the Large Facilities Capital Fund of BIS, and the Universities of Cambridge and Glasgow.

References

- [1] J. Richman and P. Burchat, *Rev.Mod.Phys.*67:893-976 (1995).
- [2] J. Gill (UKQCD Collaboration), *Nucl. Phys. B, Proc. Suppl.* 106, 391 (2002).
- [3] B. Aubert *et al*, *Phys.Rev.* D78 051101 (2008).
- [4] E. Follana *et al* (HPQCD Collaboration), *Phys.Rev.* D75 054502 (2007), hep-lat/0610092.
- [5] A. Bazavov *et al* (MILC Collaboration), *Rev.Mod.Phys.*82:1349-1417 (2010), hep-lat/0903.3598v2.
- [6] P. F. Bedaque, *Phys. Lett. B* 593 (2004) 82, arXiv:nucl-th/0402051.
- [7] D. Guadagnoli, F. Mescia and S. Simula, *Phys.Rev.* D73 114504 (2006), hep-lat/0512020.
- [8] C. T. H. Davies *et al* (HPQCD Collaboration), *Phys.Rev.* D82 114504 (2010), arXiv:1008.4018v2 [hep-lat].
- [9] K. Nakamura *et al.* (Particle Data Group), *JPG* 37, 075021 (2010) (URL: <http://pdg.lbl.gov>).
- [10] J. Koponen *et al* (HPQCD Collaboration), *PoS(Lattice 2011)286* (2011).
- [11] H. Trotter, private communication.
- [12] C. McNeile *et al* (HPQCD Collaboration), hep-lat/1004.4285v1.